B s C t - I t A t I s

L __ ,[1] H__ , ,[1] J H, ,[1] J s,[2] __ G__ ,[3] __ __ ,[3] C __ J __ ,[3] [1,4,5,6]*

[1]Center for Brain and Cognitive Sciences and Department of Psychology, Peking University, Beijing, China
[2]Department of Experimental and Applied Psychology, Vrije Universiteit, Amsterdam, 1081 BT, The Netherlands
[3]Key Laboratory of Embedded System and Service Computing (Ministry of Education), Tongji University, Shanghai 201804, China
[4]Beijing Key Laboratory of Behavior and Mental Health, Peking University, Beijing 100871, China
[5]Key Laboratory of Machine Perception (Ministry of Education), Peking University, Beijing 100871, China
[6]PKU-IDG/McGovern Institute for Brain Research, Peking University, Beijing 100871, China

Abstract: Focusing attention on a target creates a center-surround inhibition such that distractors located close to the target do not capture attention. Recent research showed that a distractor can break through this surround inhibition when associated with reward. However, the brain basis for this reward-based attention is unclear. In this fMRI study, we presented a distractor associated with high or low reward at different distances from the target. Behaviorally the low-reward distractor did not capture attention and thus did not cause interference, whereas the high-reward distractor captured attention only when located near the target. Neural activity in extrastriate cortex mirrored the behavioral pattern. A comparison between the high-reward and the low-reward distractors presented near the target (i.e., reward-based attention) and a comparison between the high-reward distractors located near and far from the target (i.e., spatial attention) revealed a common frontoparietal network, including inferior frontal gyrus and inferior parietal sulcus as well as the visual cortex. Reward-based attention speci cally activated the anterior insula (AI). Dynamic causal modelling showed that reward modulated the connectivity from AI to the frontoparietal network but not the connectivity from the frontoparietal network to the visual cortex. Across participants, the reward-based attentional effect could be predicted both by the activity in AI and by the changes of spontaneous functional

Contract grant sponsor: National Basic Research Program of China; Contract grant number: 2015CB856400; Contract grant sponsor: Natural Science Foundation of China; Contract grant number: 31170972 and 91232708.

*Correspondence to: Xiaolin Zhou, Ph.D., Department of Psychology, Peking University, Beijing, 100871, China.
E-mail: xz104@pku.edu.cn

Received for publication 3 August 2015; Revised 14 September 2015; Accepted 17 September 2015.
DOI: 10.1002/hbm.23004
Published online 29 September 2015 in Wiley Online Library (wileyonlinelibrary.com).

1000 ms interval of blank screen, the feedback frame was presented and remained on the screen for 1000 ms. The

practice trials in which the monetary feedback was replaced by response feedback (correct vs. incorrect) were provided prior to each of the two phases.

For the fMRI experiment, we included a localizer task in a separate scanning session after the test phase to identify each participant's task-relevant visual areas. Seven circles with line segment inside were presented below the xation

In the rst day, the scanning consisted of two resting-state sessions and a task session of the learning phase. The two separate runs of resting-state data, which contained 200 EPI volumes each, were acquired 3 min before (pre-learning resting-state data) and 3 min after (post-learning resting-state data) the learning phase, respectively. Spontaneous brain activity recorded in resting-state fMRI has been demonstrated to be an effective predicator of attentional performances [Carter et al., 2010; Shulman et al., 2009]. In this study, the resting-state sessions were used to explore whether the learning-induced changes of spontaneous brain activity could predict the attentional effect in the later test phase. During the resting-state scanning, participants were asked to close their eyes and keep still, and not to think about anything systematically or fall asleep for 7 min. In the second day, the scanning consisted of a session of the test phase with the main task and a session of the localizer task.

Task fMRI data

Data for the main task in the test phase were preprocessed with Statistical Parametric Mapping software SPM8 (Wellcome Trust Department of Cognitive Neurology, London, UK). For each run, the rst ve volumes were discarded to allow for T1 equilibration effects. Preprocessing was done with SPM8 default settings. Images from each run were slice time corrected and motion corrected. Different brain tissues (gray matter, white matter, and cerebrospinal signals) were segmented following the standard procedures implemented in SPM8 and were transformed into standard MNI space and resampled to $3 \times 3 \times 3$ mm^3 isotropic voxel. The data were then smoothed with a Gaussian kernel of 6 mm full-width half-maximum (FWHM) to accommodate inter-subject anatomical variability.

Resting-state fMRI data

Similar preprocessing procedures were carried out for the resting-state data in the learning phase using SPM8 and Data Processing Assistant for Resting-State fMRI (DPARSF) [Yan and Zang, 2010]. For each of the two sessions, the rst ve volumes were discarded to allow for T1 equilibration effects. The remaining images were then slice time corrected, motion corrected, and spatially normalized into standard MNI space and resampled to $3 \times 3 \times 3$ mm^3 isotropic voxel. After a linear trend of the time courses was removed, the band-pass lter (0.01 0.1 Hz) was applied to remove low-frequency drifts and high-frequency noise. White matter and cerebrospinal signal were extracted using SPM's priori masks implemented in DPARSF. The head motion parameters, mean global signal, white matter signal, and cerebrospinal uid signal were regressed out.

t t$_s$t A ss B D t

For each experimental condition in the test phrase, omissions, incorrect responses, and trials with RTs $\pm$ 3 SDs beyond the mean RT for all the correct trials were rst excluded. Mean RT of the remaining trials (95.1% of all the trials in the behavioral experiment and 90.0% in the fMRI experiment) in each condition was then computed. The error rate in each condition was calculated as the proportion of the number of omissions (including the trials in which RT was higher than 800 ms) and incorrect trials against the total number of trials in the condition (Table I).

We used $\alpha = 0.05$ as the threshold for statistical signi -

was included for each experimental condition. The six head movement parameters derived from the realignment procedure were also included. The first-level individual contrast images corresponding to the six conditions were fed to a 2 × 3 within-subject ANOVA at the second group level by employing a random-effects model (i.e., the flexible factorial design in SPM8 including an additional factor modeling the subject means). In the modeling of variance components, we allowed for violations of sphericity by modelling nonindependence across parameter estimates from the same participant and allowed for unequal variances between conditions and between participants using the standard implementation in SPM8. We defined two contrasts: "H1 > L1" and "H1 > Mean (H2 + H3)". The former contrast reflected the neural correlates of reward-based attentional capture and the latter contrast revealed the neural correlates of stimulus-driven attentional capture. To further investigate the brain-behavior correlation, a planned t contrast "H1 > L1" was computed with the behavioral interference effect (i.e., RTs at H1 minus RTs at L1) as covariate.

The AFNI program AlphaSim was used to determine our significance criterion. The smoothness was estimated using 6 mm 3dFWHM. Areas of activation were identified as significant only if they passed the threshold of $P < 0.005$ family wise (FWE)-corrected at the cluster level, which required 35 contiguous voxels, each voxel significant at $P < 0.005$ uncorrected (unless otherwise stated) [cf., Lieberman and Cunningham, 2009].

Region of interest (ROI) analysis

Although reward effects have recently been observed over the entire visual cortex [Arsenault et al., 2013], models of visual attention indicates that surround inhibition is formed to suppress the competing neural representations of the distracting objects mainly in the extrastriate cortex [Desimone and Duncan, 1995; Luck et al., 1997]. Evidence from magne-

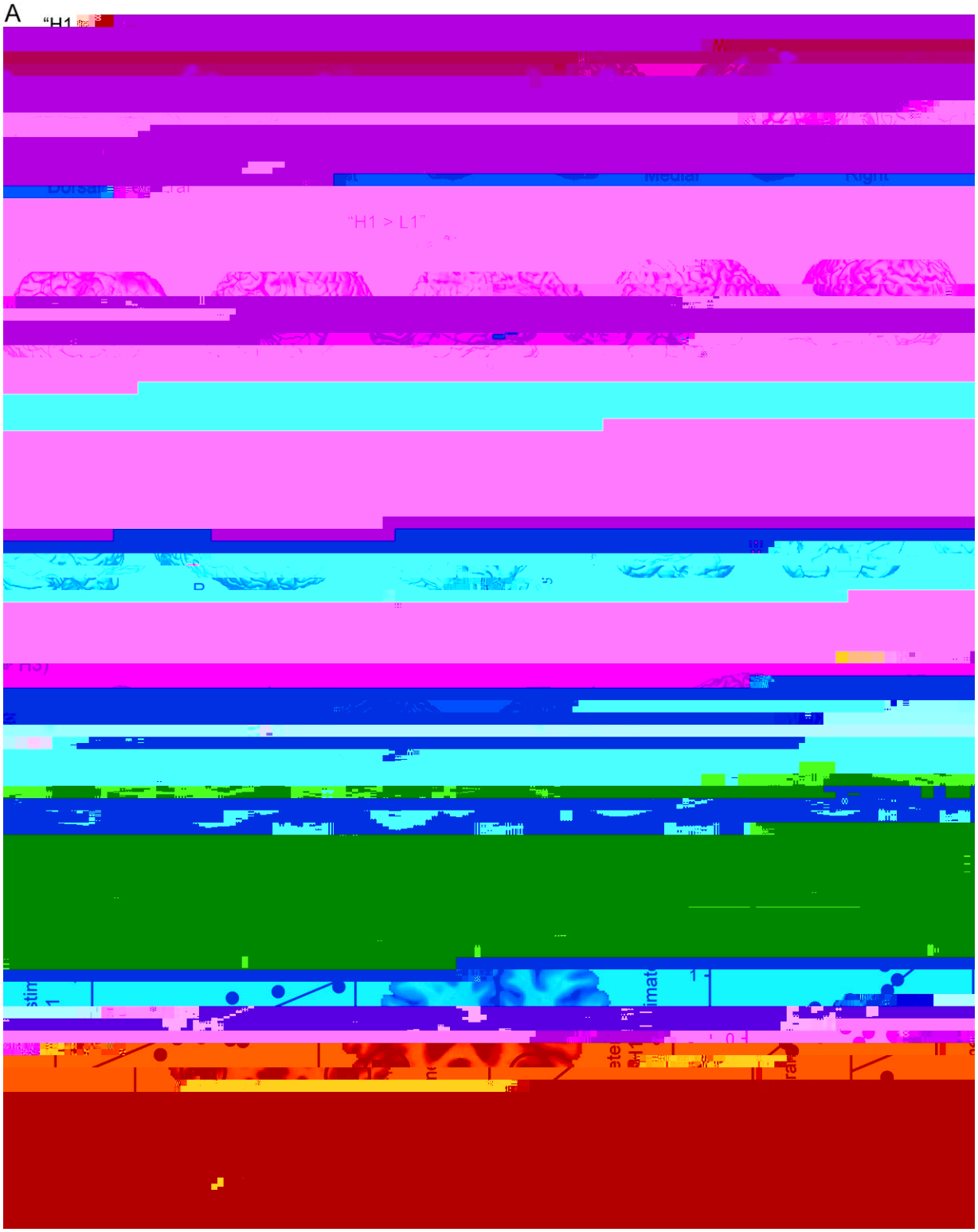
A
"H1
"H1 > L1"

Dynamic causal modeling

Different models of functional architecture and effective connectivity were compared using DCM10 implemented in SPM8. Here we used bilinear DCM, which consists of three different sets of parameters [Friston et al., 2003]: (1) the " intrinsic connectivity represents the latent connectivity between brain regions irrespective of experimental conditions; (2) the " modulatory connectivity represents the in uence of experimental conditions on the intrinsic connectivity; and (3) " input represents the driving in uence on brain regions by the experimental conditions. We extracted activation time courses (eigenvariate) from the left AI, the left inferior frontal gyrus (IFG), the left IPS and the left lateral occipital cortex (LOC) in each participant from a 3 mm sphere centered on the group peak coordinates revealed by the contrast " H1 > L1 (see " Results). The connectivity between IFG/IPS and the visual cortex (LOC in this study) was constructed based on previous models of the stimulus-driven attentional network [Vossel et al., 2012]. The intrinsic connectivity between AI and IFG/IPS was also speci ed because of AI's involvement in reward-based attention and its correlation with the behavioral interference effect (see " Results). Given the important role of AI in representing stimulus salience [Uddin, 2015], we hypothesized that the reward-based salience is represented in AI and then projected to the frontoparietal network (IFG and IPS), which in turn modulates the neural activity in LOC. Based on this hypothesis, we constructed 8 model families characterized by three independent factors: the presence or absence of the intrinsic connectivity from LOC to AI, the direction (i.e., bilateral or unilateral) of intrinsic connectivity between AI and the frontoparietal network, and the direction (i.e., bilateral or unilateral) of intrinsic connectivity between the frontoparietal network and LOC (Fig. 4A). AI received the salience input (the reward-based salience, H1 vs. L1) in all the model families, whereas LOC received the visual input in the model families in which it had in uence on other areas. Each model family contained nine single models that share the same driving input and intrinsic connectivities, but differed in the structure of the modulatory connectivity exerted by reward. Table III summarized the structure of the modulatory connectivity in the nine models. To test our hypothesis concerning reward-based attention, only H1 and L1 were included in the modeling. It should be noted that for families containing bilateral intrinsic connectivity, the H1 and L1 conditions were speci ed to modulate on both directions.

ABLE III. s t , t s t t DCM

Models	1	2	3	4	5	6	7	8	9
AI IFG	1	1	0	0	0	0	1	1	0
AI IPS	1	1	0	1	1	0	0	0	0
IFG - LOC	1	0	1	0	0	0	1	0	1
IPS - LOC	1	0	1	1	0	1	0	0	0

Notes: AI: anteriobr insula; IFG: inferior frontal gyrus; IPS: intraparietal sulcus; LOC: lateral occipital cortex; 1: presence, 0: absence.

These models and model families were then compared using the Bayesian Model Selection (BMS), which uses a Bayesian framework to compute the " model evidence of each model, representing the trade-off between model simplicity and model tness [Penny et al., 2004]. Here, BMS was implemented using random-effect analysis (i.e., assuming that the model structure may vary across participants) that is robust to the presence of outliers [Stephan et al., 2009]. Based on the estimated model evidence for each model, random effect BMS calculates the exceedance probability, that is, the probability of each model being more likely than any other model. When comparing model families, all models within a family were averaged using Bayesian Model Averaging, and the exceedance probabilities were calculated for each model family [Penny et al., 2010]. Model parameters were estimated based on the averaging of the winning family and were tested with one-sample t tests.

F . 3.

Results of the whole brain analysis for the test phase. **A**: Blue: the activations revealed by the contrast "H1 > Mean (H2 + H3)". Red: the activations revealed by the contrast "H1 > L1." Purple: the common activated regions of the two networks. Green: the brain activations revealed by the contrast "H1 > L1" exclusively masked by the contrast "H1 > Mean (H2 + H3)". Statistical parametric map was shown at the threshold of $P < 0.005$ FWE-corrected at cluster level, $P < 0.005$ uncorrected at voxel level (H1: high-reward distractor, location 1; H2: high-reward distractor, location 2; H3: high-reward distractor, location 3; L1: low-reward distractor, location 1). **B**: AI was activated by the contrast "H1 > L1" when the RT difference between H1 and L1 conditions were included as covariates (middle panel). Parameter estimates were extracted from the two clusters. Scatter plots (with best-fitting regression lines) illustrates the difference of the parameter estimates between H1 and L1 conditions as a function of the RT difference (left and right panels). In the right panel, the correlation was still significant after the outlier (the bottom left dot) is excluded from the data ($R^2 = 0.59$). Thus, we keep all the data points in the plot. Note that the bottom left dot in the right panel was identified as the only outlier because the activity strength (the value of parameter estimates) of this dot in the right AI was beyond −3SD of the group mean. No outlier was found in the left panel.

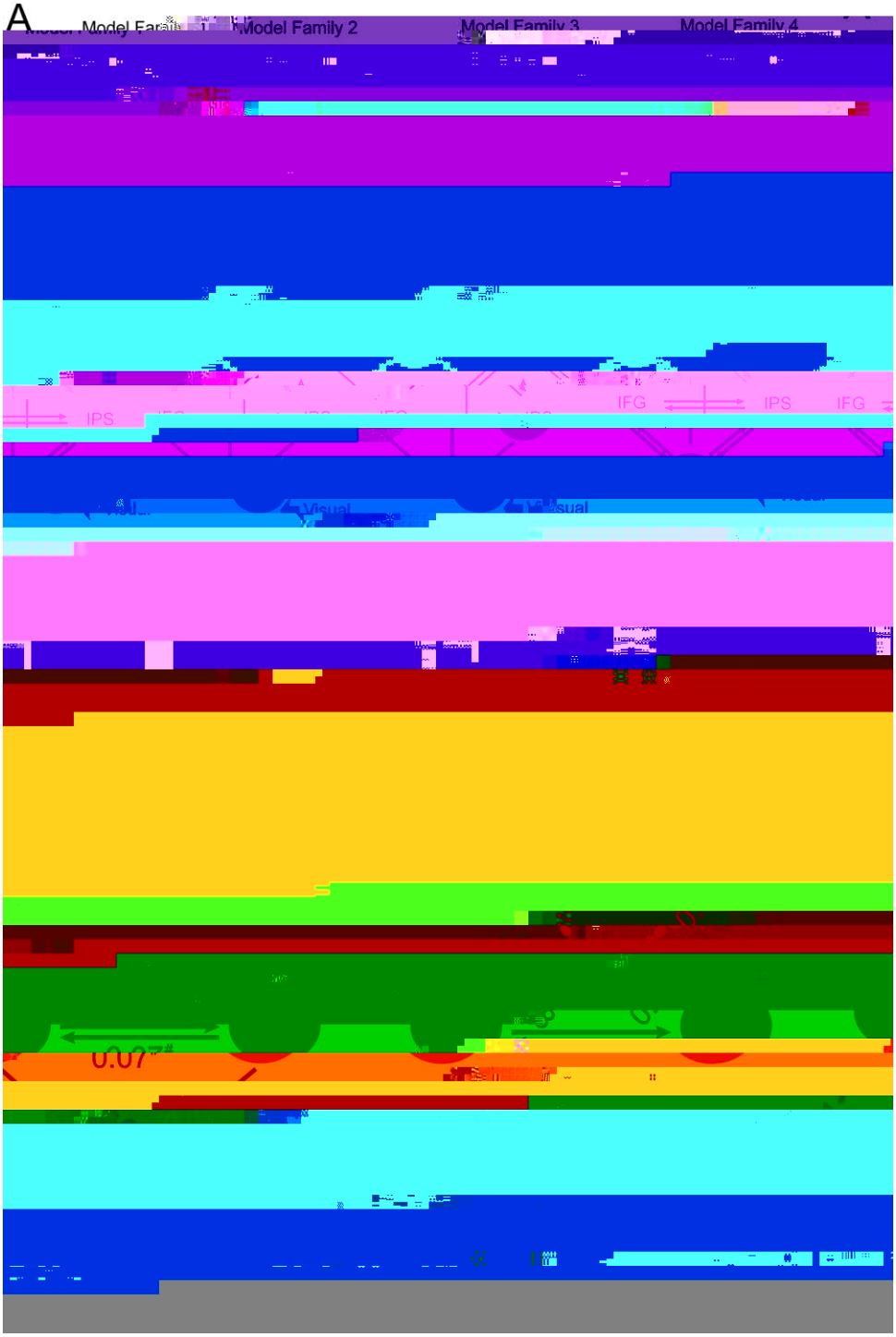

F . . 4.

The dynamic causal modeling (DCM) analysis for AI and the fronto-parietal network. **A**: The structure of 8 model families (left hemisphere). These model families differed in terms of the presence or absence of the intrinsic connectivity from LOC to AI, the direction of the intrinsic connectivity between AI and IFG/IPS, the direction of the intrinsic connectivity between IFG/IPS and LOC, and the input. Each model family contained nine models, which differed in the specific pathway(s) that modulated by reward (H1 vs. L1, see Table III). **B**: The exceedance probabilities of the eight model families (left panel) and the single models (right panel). The single models from the eight model families were ordered in consistence with Table III. **C**: The estimated DCM parameters of the average model of the winning family (* *P*

Resting-state analysis

According to our hypothesis, the salience of the reward-associated stimulus was increased after learning. However, given the lack of behavioral differences between high- and low-reward targets in the learning phase, it was not clear when the reward-based salience was acquired. To overcome this de cit, we took advantage of the resting-state data and examined whether the functional connectivity (FC) in the post-learning session could predict participants' interference effect in the test phase. A recent study suggested that the VS, a subcortical area that represents reward value [Sescousse et al., 2010], interacted with the AI in directing attention to reward-related stimulus [Rothkirch et al., 2014]. We hence expected that the behavioral interference effect could be predicted by FC between VS and AI. The FC analysis was carried out using the Resting-State fMRI Data Analysis Toolkit (REST; http://www.restfmri.net/) [Song et al., 2011]. The coordinates of the bilateral AI were based on the results of whole-brain analysis, and the coordinates of the bilateral VS (left: $x = -12$, $y = 9$, $z = -9$; right: $x = 9$, $y = 6$, $z = -9$) were based on a previous study of reward processing [Sescousse et al., 2010]. We created spherical seeds centered on the coordinates of the ROIs with a radius of 6 mm. To produce a participant-level FC map, we computed the mean time series across all voxels in these areas and performed correlation analysis between the AI and the VS for each participant. These FC maps were then converted to z-FC maps by conducting Fisher z score transformations. These analyses were performed for both the pre-learning and the post-learning data. Next, we performed correlation analysis between the Fisher z scores and participants' interference effect for both the pre-learning and the post-learning sessions. Partial correlation was also performed after the Fisher z scores in the pre-learning session had been controlled. We further calculated the change of FC after learning by subtracting the Fisher z scores in the pre-learning session from the scores in the post-learning session and examined correlation between the change of FC and the behavioral interference effect.

E L

B D t

Given that neither error rates nor RTs in the learning phase showed signi cant differences between experimental conditions, the following report focuses on RTs and error rates in the test phase (Table I).

For the behavioral experiment, repeated-measures analysis of variance (ANOVA) on RTs showed a main effect of location, $F\ (2,\ 26) = 11.20$, $P < 0.001$, $\eta_p^2 = 0.463$, and an interaction between distractor type and location, $F\ (2,\ 26) = 4.63$, $P < 0.05$, $\eta_p^2 = 0.263$, but no main effect of distractor type, $F < 1$. Separate ANOVAs on the location effect were carried out for the low-reward and high-reward distractors, respectively. For the low-reward distractor, RTs at the three locations (L1: 484 ms, L2: 483 ms, L3: 480 ms) did not differ from each other, $F < 1$. For the high-reward distractor, there was a signi cant location effect, $F\ (2,\ 26) = 11.74$, $P < 0.001$, $\eta_p^2 = 0.474$. Further pairwise comparisons with Bonferroni correction showed that RTs at H1 (494 ms) was longer than RTs at H2 (478 ms) and H3 (474 ms), with no difference between the latter two: H1 vs. H2, $P < 0.05$, 95% con dence interval (CI) [3.5, 28.8]; H1 vs. H3, $P < 0.01$, 95% CI [6.9, 33.5]; H2 vs. H3, $P > 0.1$, 95% CI [−6.1, 14.2]. The interaction between distractor type and location was also examined from the other direction. Paired t tests were carried out for the reward effects at each of the three locations. The results showed that RTs at H1 was longer than RTs at L1, $t\ (13) = 2.14$, $P = 0.052$, 95% CI [−0.1, 20.4], whereas RTs at H2 did not differed from RTs at L2, $t\ (13) = 1.16$, $P > 0.1$, 95% CI [−13.7, 4.2], and RTs at H3 was shorter than RTs at L3, $t\ (13) = 2.52$, $P < 0.05$, 95% CI [−11.6, 0.9] (Fig. 1C, left panel). When the H3 and L3 conditions were excluded, the 2 (Reward: high vs. low) × 2 (Location: 1 vs. 2) ANOVA still showed an interaction between reward type and location, $F\ (1,\ 13) = 4.72$, $P < 0.05$, $\eta_p^2 = 0.266$, indicating that the interaction between reward and location was driven at least partly by the delayed RTs at H1 relative to L1. The ANOVA on error rates showed only a trend of interaction between reward type and location, $F\ (2,\ 26) = 2.73$, $P = 0.084$, η

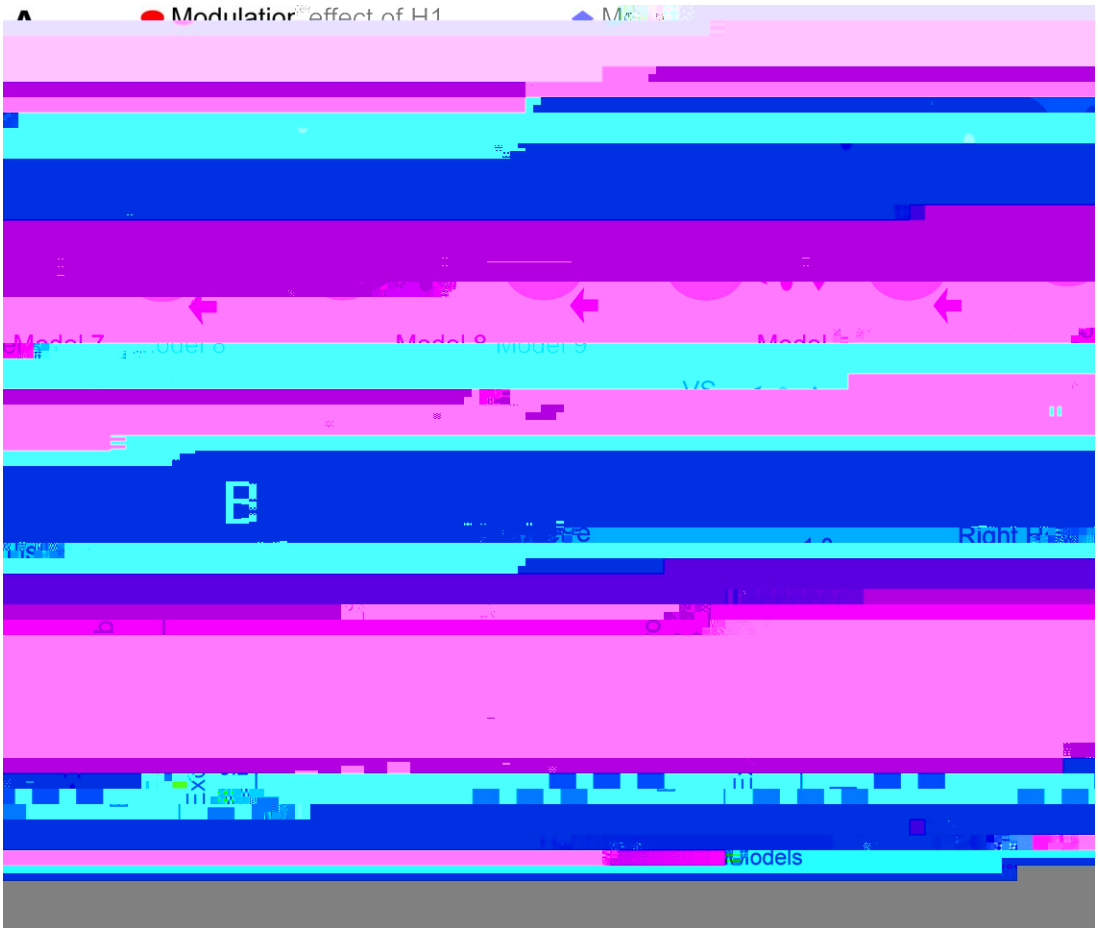

F . . 5.

The DCM analysis for AI and VS. **A**: The structure of 12 models with different intrinsic connectivities and modulatory connectivities. **B**: The exceedance probabilities of the 12 models in the left (left panel) and the right (right panel) hemisphere. [Color figure can be viewed in the online issue, which is available at wileyonlinelibrary.com.]

no difference between H2 and H3, $P > 0.1$, 95% CI [−7.7, 10.5] (Fig. 1C, right panel). For the reward type, there was only a signi cant difference between H1 and L1, $t(16) = 2.89$, $P < 0.05$, 95% CI [1.8, 11.7], but not between H2 and L2 or between H3 and L3, both $P > 0.1$, 95% CI [−9.1, 4.4] and [−5.8, 5.4]. ANOVA on error rates did not show any signi cant effects, all $P > 0.1$.

We noticed that the effects (i.e., H1 > H2, H1 > H3) in terms of RTs, as well as in terms of neural activity in the visual cortex (shown in the imaging data below), were not as strong as in the behavioral experiment, although qualitatively the patterns in the two experiments were similar. This reduction in the effect size may be due to scanner noise, vibration and unfamiliar body gestures in the scanner [cf. Anderson et al., 2014]. We believe that the reduction in RT effect sizes have not signi cantly undermined our main arguments, for these arguments and most of our analyses of neural data were primarily based on the effects between H1 and L1, which were robust in both the behavioral and the fMRI experiments.

I D t

Reward-based attentional capture in the visual cortex

We rst examined whether the effect of reward-based attentional capture in the test phase was manifested in visual cortex. Parameters estimates of the six experimental conditions were extracted from the left and the right extrastriate cortex identi ed in our localizer task. The 2 (Hemisphere: left vs. right) × 2 (Reward: high vs. low) × 3 (Location: 1, 2 vs. 3) ANOVA on the parameter estimates revealed only a signi cant interaction between reward and location, $F(2, 32) = 6.20$, $P < 0.01$, $\eta_p^2 = 0.279$. For the low-

reward distractor, the ANOVA on the location effect showed that the neural activity (collapsed across the left and the right extrastriate cortex) at L1, L2, and L3 did not differ from each other, $F\ (2,\ 32) = 1.99$, $p > 0.1$, but there was a linear trend, $F\ (1,\ 16) = 4.32$, $P = 0.054$, $\eta_p^2 = 0.213$, with the neural activity increasing from L1 to L2 and to L3. For the high-reward distractor, the location effect was

and AI. The VS was de ned in the same way as in the resting state. Nine Models with different intrinsic connectivities and modulatory connectivities were constructed and compared, but no model won in the BMS (Fig. 5). This indicated that the reward system may not be extensively involved in reward-based attentional capture in the test phase.

Learning-induced changes in spontaneous brain connectivity

For the pre-learning session, the FC between AI and VS did not correlate with the behavioral interference effect in the test phase, left hemisphere: Pearson $r = -0.29$, $P > 0.1$, right hemisphere: $r = -0.00$, $P > 0.1$ (Fig. 6A). In contrast, for the postlearning session, there were strong positive correlations between FC and the behavioral interference effect, left hemisphere: $r = 0.63$, $P < 0.01$, right hemisphere: $r = 0.53$, $P < 0.05$ (Fig. 6B). After FC in the pre-learning session had been controlled, the partial correlation analysis still showed positive correlations between the behavioral interference effect and FC in the post-learning session, left hemisphere: $r = 0.62$, $P < 0.05$, right hemisphere: $r = 0.64$, $P < 0.01$. Moreover, there were also signi cant positive correlations between the change of FC after learning and the behavioral interference effect, left hemisphere: $r = 0.61$, $P < 0.01$, right hemisphere: $r = 0.57$, $P < 0.05$ (Fig. 6C). These results suggested that the reward-based attentional capture in the test phase could be predicted by the spontaneous FC between AI and VS after learning.

DI C ION

In this fMRI study, we investigated the neural mechanism of reward-based attention by distinguishing reward- and attention-related signals. We found that IFG, IPS, and the visual cortex are commonly activated in reward-based and stimulus-driven attention, whereas AI was only activated in reward-based attention. Reward enhanced the effective connectivity from the salience network (e.g., AI) to the attention network (e.g., IFG/IPS), but not the connectivity from IFG/IPS to the visual cortex. Moreover, the reward-based attentional effect could be predicted both by

reward distractor interfered with the target processing when it was located adjacent to the target (0.9°) but did not cause interference when it was located further away from the target (2.1 4.5°). The low-reward distractor in far distances failed to cause interference as a result of the surround inhibition, which emerged around 1.54° from the target [Mounts, 2000b]. In contrast, the high-reward distractor caused interference in both near (0.9°) and far locations (2.1°). However, this interaction between reward and location occurred only when attention was initially focused on the target, for example, when the location of the target was highly predictable, but disappeared when there was no initial attention on the target, for example, when the location of the target was unpredictable [Wang et al., 2014]. Given that the initial attention on the target is indispensable for the formation of surround inhibition [Cutzu and Tsotsos, 2003], the interference effect induced by the high-reward distractor at 2.1° from the target was attributed to a " breakthrough of the surround inhibition rather than a simple extended interference effect [Wang et al., 2014].

In a similar vein, here we increased the distance (1.6°) between the target and the distractor to ensure that the reward-associated distractor fell into this inhibitory region. Results in both the behavioral experiment and the fMRI experiment showed that low-reward distractors induced comparable RTs when they were located in this inhibitory region, whereas high-reward distractor induced increased RTs at H1 than at H2 and H3. Moreover, when data from the two experiments were collapsed, Bonferroni corrected comparisons showed that RTs at H1 was longer than RTs in the other conditions (H2, H3, L1, L2, L3), all $P < 0.05$, whereas RTs in the other conditions did not differ from each other, all $P > 0.1$ (except for a marginal signi cance, $P = 0.08$, when comparing RTs at H3 and L1). These results are consistent with our previous ndings [Wang et al., 2014], indicating that only the high-reward distractor near the target (H1) captured attention and interfered with target processing. At the neural level, the activity in the extrastriate cortex showed a similar pattern, providing new evidence for the argument that reward could break through the center-surround inhibition [Wang et al., 2014]. In a broader sense, this nding is also in line with the idea that the modulatory effects on visual cortex of top-down attention and the value of stimuli may engage an overlapping neuronal selection mechanism [Maunsell, 2004; Stanisor et al., 2013].

In this study, despite that the RTs at different locations were comparable for the low-reward distractors, neural activity in the early visual cortex showed a linear increase with increasing distance from the target, indicating a recovery from surround inhibition. This recovery effect was also reported in previous studies on surround inhibition [Boehler et al., 2009; Hopf et al., 2006]. According to these studies, the surround inhibition manifests near the attentional focus and attenuates with the increasing distance from the attentional focus. For example, Hopf et al. [2006; 2009] showed that only the stimulus adjacent to the attended target (1.35° in visual angle) was suppressed in the early visual cortex and the processing of stimulus in the distant locations (2.15°) was recovered, even though RTs did not differ between locations. However, in contrast to a robust recovery in Hopf et al. [2006; 2009], the recovery of the surround inhibition for the low distractor in the current study was relatively weak (only a linear trend from 1.6° to 4°). This discrepancy could be attributed to the difference in stimulus arrays. Distractors were located in a single quadrant of the visual space in previous studies [Boehler et al., 2009; Hopf et al., 2006], but were located in both hemispheres in this study. Given that between-hemisphere distraction is more easily to inhibit than within-hemisphere distraction [Alvarez and Cavanagh, 2005; Wei et al., 2013], the inhibitory region across hemispheres might be larger than the region within a hemisphere.

It should be noted that the recovery from surround inhibition in the early visual cortex was observed only for the low-reward but not for high-reward distractor. While neural representation for the low-reward distractor increased linearly from near to far locations, neural representation for the high-reward distractor did not show this pattern and even decreased from H2 to H3. This asymmetry, together with the shorter RTs at H3 relative to L3 in the behavioral experiment, may indicate that another neural and psychological process was taking effect for the high-reward distractor, that is, the active suppression of high versus low salient distractor [Geng, 2014]. The active suppression functions to prevent attentional allocation to task-irrelevant stimulus, especially when this stimulus is characterized with high salience [Geng, 2014; Sawaki et al., 2012]. In this study, because the target location was xed and a singleton distractor was present in every trial, the active suppression mechanism was triggered to suppress the distractor; this suppression could be more powerful for the distractor with high reward-based salience compared with the distractor with low reward-based salience. The electrophysiological index of this active suppression was observed when the reward-associated distractor was rapidly rejected, demonstrating the active suppression of the reward-associated distractor [Qi et al., 2013; Sawaki et al., 2015]. Given that the strength of this active suppression is determined by the representational distance between the target and the distractor [Geng, 2014], the distractor located far from the target (H3, H2) is more effectively suppressed than the distractor near the target (H1). In this way, although the distractor at H1 " broke through the surround inhibition, the distractors at H2 and H3 suffered from active suppression and did not receive adequate representation in the extrastriate cortex.

Previous studies did not draw consistent conclusions regarding the neural basis of reward-based attention. In an event-related potential study, Hickey et al. [2010] showed

that the effect of attentional orienting to reward-associated stimulus correlated with the amplitude of medial frontal negativity (MFN) that could be localized at the anterior cingulate cortex (ACC). The activity in ACC also correlated with the attentional orienting effect, leading to the argument that reward increases salience by the mediation of ACC.

this attention is controlled by the interaction between the dorsal and ventral networks [Vossel et al., 2012]. Second, although TPJ is part of the ventral network, it is not always activated in studies investigating stimulus-driven attention. For example, Kincade et al. [2005] found that TPJ did not exhibit greater response to salient task-irrelevant color singleton than to other stimuli. The authors thus claimed that TPJ is involved only in involuntary shift to behaviorally relevant stimuli. A related argument was that a lter determines the input to TPJ and whether a distractor in visual search could pass through this lter depends on whether it meets the de nition of the target [Shulman et al., 2003]. It is possible that the task-irrelevant distractor in this study could not pass through this lter and thus could not activate TPJ.

One might also argue that the attentional network revealed through the distance effect [H1 vs. Mean (H2 + H3)] was not exclusively responsible for stimulus-driven attention since the stimuli at the three locations were all reward-related and reward may have differential impacts upon the processing of the stimuli at different locations. Although we could not completely rule out this possibility, we believe that the frontoparietal network revealed in the contrast subserved at least the attentional orienting to the reward-associated distractor. First, this network accords well with the stimulus-driven network revealed in previous studies with stimuli presented in a no-reward context [Vossel et al., 2012]. Second, according to our DCM, the effective connectivity from this network to the visual cortex was not mediated by reward, excluding a role of this network in representing reward information. Last, the involvement of AI in the reward-based effect but not in the distance effect additionally con rmed the functional dissociation between the frontoparietal network and AI.

CONCL ION

Our results revealed distinct roles of AI and the stimulus-driven network in reward-based attention. Associating rewarding information to a stimulus increases the salience of that stimulus and this reward-based salience is represented in AI, which projects this information onto the stimulus-driven attentional network and enables the reward-associated distractor to break through the center-surround inhibition in the visual cortex.

ACKNO LEDGMEN

The authors thank Dr. Xilin Zhang and Dr. Sheng Li for suggestions concerning the design of the fMRI experiment, and Miss Yunyan Duan and Miss Yiyuan Wang for help with the test of participants. This study was supported by the National Basic Research Program (973 Program: 2015CB856400) from the Ministry of Science and Technology of China. The authors declare no con ict of interest.

EFE ENCE

Alvarez GA, Cavanagh P (2005): Independent resources for attentional tracking in the left and right visual hemi elds. Psychol Sci 16:637 643.

Anderson BA (2013): A value-driven mechanism of attentional selection. J Vis 13:7 7.

Anderson BA, Yantis S (2013): Persistence of value-driven attentional capture. J Exp Psychol Hum Percept Perform 39:6 9.

Anderson BA, Laurent PA, Yantis S (2011): Value-driven attentional capture. Proc Natl Acad Sci U S A 108:10367 10371.

Anderson BA, Laurent PA, Yantis S (2014): Value-driven attentional priority signals in human basal ganglia and visual cortex. Brain Res 1587:88 96.

Arsenault JT, Nelissen K, Jarraya B, Vanduffel W (2013): Dopaminergic reward signals selectively decrease fMRI activity in primate visual cortex. Neuron 77:1174 1186.

Awh E, Belopolsky AV, Theeuwes J (2012): Top-down versus bottom-up attentional control: A failed theoretical dichotomy. Trends Cogn Sci 16:437 443.

Berridge KC, Robinson TE (1998): What is the role of dopamine in reward: Hedonic impact, reward learning, or incentive salience? Brain Res Rev 28:309 369.

Boehler CN, Tsotsos JK, Schoenfeld MA, Heinze HJ, Hopf JM (2009): The center-surround pro le of the focus of attention arises from recurrent processing in visual cortex. Cereb Cortex 19:982 991.

Dalton KM, Kalin NH, Grist TM, Davidson RJ (2005): Neural-cardiac coupling in threat-evoked anxiety. J Cogn Neurosci 17: 969 980.

Desimone R, Duncan J (1995): Neural mechanisms of selective visual attention. Ann Rev Neurosci 18:193 222.

Downar J, Crawley AP, Mikulis DJ, Davis KD (2000): A multimodal cortical network for the detection of changes in the sensory

Stanisor L, van der Togt C, Pennartz CM, Roelfsema PR (2013): A uni ed selection signal for attenion and reward in primary visual cortex. Proc Natl Acad Sci U S A 110:9136 9141.

Stephan KE, Penny WD, Daunizeau J, Moran RJ, Friston KJ (2009): Bayesian model selection for group studies. Neuroimage 46: 1004 1017.

Theeuwes J (1991): Cross-dimensional perceptual selectivity. Percept Psychophy 50:184 193.

Theeuwes J (1992): Perceptual selectivity for color and form. Percept. Psychophy 51:599 606.

Uddin LQ (2015): Salience processing and insular function and dysfunction. Nature Rev Neurosci 16:55 61.

Vossel S, Weidner R, Thiel CM, Fink GR (2009): What is " odd in Posner's location-cueing paradigm? Neural responses to unexpected location and feature changes compared. J Cogn Neurosci 21:30 41.

Vossel S, Weidner R, Driver J, Friston KJ, Fink GR (2012): Deconstructing the architecture of dorsal and ventral attention systems with dynamic causal modeling. J Neurosci 32:10637 10648.

Wang L, Yu H, Zhou X (2013): Interaction between value and perceptual salience in value-driven attentional capture. J Vis 13:5.

Wang L, Duan Y, Theeuwes J, Zhou X (2014): Reward breaks through the inhibitory region around attentional focus. J Vis 14:2.

Wei P, Kang G, Zhou X (2013): Attentional selection within and across hemispheres: Implications for the perceptual load theory. Exp Brain Res 225:37 45.

Yan C, Zang Y (2010): DPARSF: A MATLAB Toolbox for " Pipeline Data Analysis of Resting-State fMRI. Front Syst Neurosci 4:13.

Yantis S, Jonides J (1984): Abrupt visual onsets and selective attention: Evidence from visual search. J Exp Psychol Hum Percept Perform 10:601 621.

Yantis S, Jonides J (1990): Abrupt visual onset and selective attention: Voluntary versus automatic allocation. J Exp Psychol Hum Percept Perform 16:121 134.

Yu R, Zhou W, Zhou X (2011): Rapid processing of both reward probability and reward uncertainty in the human anterior cingulate cortex. PLoS One 6:e29633.